Monte Carlo simulations of a model ultra-thin magnetic bilayer

2007 J. Phys.: Condens. Matter 19 456223

(http://iopscience.iop.org/0953-8984/19/45/456223)

IOP PUBLISHING JOURNAL OF PHYSICS: CONDENSED MATTER

J. Phys.: Condens. Matter **19** (2007) 456223 (14pp) doi:10.1088/0953-8984/19/45/456223

Monte Carlo simulations of a model ultra-thin magnetic bilayer

Tingxi Tan[1] **and A B MacIsaac**

The Department of Applied Mathematics, The University of Western Ontario, London, ON, N6A 5B9, Canada

Received 1 August 2007, in final form 2 October 2007
Published 22 October 2007
Online at stacks.iop.org/JPhysCM/19/456223

Abstract

Using Monte Carlo simulation we consider a model of an ultra-thin magnetic bilayer to study the effects of a second layer on the striped patterns found in monolayers with perpendicular magnetic moments. To make the problem tractable we consider a static lower layer, ordered antiferromagnetically, and coupled via a ferromagnetic exchange interaction to the top layer. The moments in the top layer are coupled by both a short-range exchange interaction and a long-range dipolar interaction. Extensive simulations reveal that varying the strength of the coupling between the two layers yields a novel phase diagram. We show that there exists a region in phase space where the ground state is a rotated stripe phase, where stripes form along the diagonal of the underlying lattice. There is also a small region in phase space where for large interplanar coupling the ground state is a zipper phase.

(Some figures in this article are in colour only in the electronic version)

1. Introduction

The nature of layered magnetic systems is currently an extremely active field of materials research. Such systems can exhibit novel physical properties, which are quite distinct from those of the bulk material [1]. The exploitation of these properties for technological uses, such as data storage, is widespread, hence the need to continually refine our understanding of such systems [2, 3]. For example, research into magnetic bilayers to study exchange bias phenomena is very active [4–8]. Similarly there has been considerable interest in the properties of ultra-thin (single-layer) magnetic films, which have been shown to have subtle, interesting phase behaviour [1, 9].

If one were to consider a model for a magnetic bilayer, experimental evidence would require one to consider the effects of a number of interactions which are believed to be important in describing the underlying physics [1]. In particular, the competition between the magnetic dipole–dipole interaction and the exchange interaction is accepted as being

[1] Present address: Department of Computer Science, The University of Calgary, Calgary, AB, T2N 1N4, Canada.

responsible for the pattern formation observed in magnetic monolayers. The nature of the exchange interaction between layers is an open problem in the aforementioned studies of exchange bias. It is also an interaction that can be partially controlled by modifying how a bilayer is constructed and therefore might be used in the future to design materials with predefined properties. Therefore, such an interaction should be included in any reasonable model. The effects of an applied field are relevant, as an applied field is often used to manipulate local magnetic properties within a device. Crystalline electric fields and magnetic surface anisotropy are important as they select preferential magnetic axes along which the system may order. A practical consideration of this is that memory device manufacturers are able to increase the capacity (storage density) of their devices by using systems with uniaxial magnetic moments oriented perpendicular to the layers of the devices. In addition, the number of components the spins can have is relevant, as it can have a fundamental effect on the nature of any critical phenomena observed in such systems. Taking all these details into consideration, a useful starting point for a model would be the Hamiltonian

$$\mathcal{H} = \sum_{\langle i,j \rangle} J_{ij} \vec{\sigma}_i \cdot \vec{\sigma}_j + \frac{g}{2} \sum_{i \neq j} \left(\frac{\vec{\sigma}_i \cdot \vec{\sigma}_j}{r_{ij}^3} - 3 \frac{(\vec{\sigma}_i \cdot \vec{r}_{ij})(\vec{\sigma}_j \cdot \vec{r}_{ij})}{r_{ij}^5} \right) + \vec{H} \cdot \sum_i \vec{\sigma}_i + \sum_i \sum_{\alpha\beta} A_{\alpha\beta} \sigma_i^\alpha \sigma_i^\beta. \quad (1)$$

In equation (1), $\vec{\sigma}_i$ is the magnetic moment at displacement vector $\vec{r}_i$. The first term is a general exchange interaction with a sum over all nearest neighbours. The second term is the long-range, dipole–dipole interaction of strength g, with $\vec{r}_{ij} = \vec{r}_i - \vec{r}_j$. The third term treats an applied magnetic field, $\vec{H}$, and the final term parametrizes any localized on-site anisotropy. Each of these terms is discussed in detail by De'Bell *et al* [9].

As one can see, such a general model has many parameters, which is in part why such systems can exhibit such a wide array of physical phenomena. Typically, one tries to limit the number of free parameters in order to make the problem more tractable. The focus of this work is on how the addition of a second layer affects the pattern formation that has been observed both experimentally and in simulations for monolayers with perpendicular magnetic moments. Therefore, we will assume that the magnetic anisotropy is such that the magnetic moments are uniaxial and oriented along the direction perpendicular to the plane of the film. For data storage purposes, perpendicular spins are relevant as they allow greater areal density. The critical temperature for such monolayer systems is predominantly defined by the strength of the exchange interaction, but, as stated above, the pattern formation is the result of frustration introduced by the competition between the dipole–dipole and the exchange interaction. Thus it is essential that we include both these interactions within the upper layer. Quite often the second layer is composed of a different material than that of the first. This means the strength of the exchange interaction within the two layers may differ and thus the critical temperatures of the two layers can be distinct. In this paper we will consider the case where the two layers have well separated Néel temperatures, and where the Néel temperature of the lower layer is substantially higher than that of the upper layer. For our purposes it will suffice to assume that the second layer is fully ordered and is static in the temperature region of interest. The coupling between the layers is dominated by the exchange interaction, and the dipole–dipole interaction between spins in different layers is less significant and can initially be ignored. Given these considerations and for the purposes of this paper, we will consider a magnetic bilayer, where the lower layer consists of uniaxial magnetic moments, which are assumed to be static and arranged as a pure antiferromagnet (AA state). On top of this static layer we assume is a second magnetic layer with the two lattices perfectly matched. Such an arrangement, two

layers of a simple cubic system, is not typical of real bilayer systems. However, given that we have initially assumed a static lower layer, the model is an appropriate first approximation to the case of two layers of an fcc or bcc lattice, where the net interaction between a spin in the upper layer and its nearest neighbours in the lower layer is antiferromagnetic. Conceptually, it is easier to think of this as two layers of a simple cubic system; however, for future work with a fully dynamic lower layer which includes the interlayer dipolar interaction we will be unable to make this analogy.

The moments in this upper layer couple within the layer via a long-range, dipole–dipole interaction of strength g, as well as a nearest-neighbour exchange interaction of strength J. The two layers are coupled via a nearest-neighbour exchange interaction of strength J_s. The Hamiltonian for the system can be written as

$$\mathcal{H} = -J \sum_{\langle ij \rangle} \sigma_i \sigma_j + g \sum_{i,j} \sigma_i \Gamma_{ij} \sigma_j - J_s \sum_i \sigma_i \sigma_i^{\mathrm{s}}, \tag{2}$$

where $\langle i, j \rangle$ in the first term indicates a sum over all pairs of nearest-neighbour spins i, j in the upper layer, $\sigma_i = \pm 1$ is the magnetic moment at site i in the upper layer and J is the strength of the exchange interaction within this layer. The second term is a long-range, dipole–dipole interaction, again only between spins in the upper layer and the sum is over all pairs of spins. We make use of Ewald sums to account for the long-range nature of the interaction; the exact form of Γ_{ij} and other details related to the Ewald summation are as given by Booth *et al* [10]. In addition to these two intraplanar interactions, the last term is the exchange coupling between the static lower layer and the upper layer. σ_i^{s} is the magnetic moment of the spin at lattice site i in the lower layer and the sum in this term is over all lattice sites. For this paper $\sigma_i^{\mathrm{s}} = (-1)^{n_x + n_y}$, where n_x and n_y are integers defined by the displacement vector for spin σ_i, $r_i = a(n_x \hat{x} + n_y \hat{y})$, and where a is the lattice spacing. For such a static lower layer the Hamiltonian is invariant under the transformation $J_s \to -J_s$, and hence we will treat only the case of positive J_s. As the spins in the lower layer are assumed to be fixed, the last term in equation (2) can, of course, be rewritten in terms of a staggered external magnetic field acting on the spins in the upper layer. We have chosen to write it in the form shown in equation (2) to emphasize the connection with the layered systems that motivate this work. As indicated above, the interplay between the intralayer interactions and the interlayer interaction is expected to play a fundamental role in determining the magnetic structures in layered systems. As we will show below, the addition of the symmetry breaking induced by the presence of the lower layer in our present model to the inherent frustration of the upper layer with dipolar and exchange interactions, is sufficient to modify the observed pattern formation. If one were to assume a static, ferromagnetic lower layer, the Hamiltonian would be equivalent to that for a monolayer in an applied field, which has been considered previously [11].

Models of a monolayer with the first two interactions have been studied extensively and a review of this work can be found in De'Bell *et al* [9] and the works cited therein. In the work presented here the ratio of J to g has been fixed at $J/g = 8.9$, which has been shown previously to lead to an ordered ground state, for a monolayer, of stripes of width eight spins parallel to a lattice axis (axial stripes) [12]. Such an axial stripe phase is shown schematically in figure 1(a). Additional ratios of J/g, with different stripe widths, but still with axial stripe ground states, have also been simulated, with similar results.

Tang and Sun [13] previously considered a related model at zero temperature. In their model system the exchange interactions within the planes and between the planes of the multilayer were considered to be the same ($J_s = J$), and the ratio of the strength of this exchange interaction and the strength of the dipole–dipole interaction was allowed to vary. They used a truncation method to calculate the dipole–dipole interaction between all spins in all layers. For this model they calculated the energies for axial stripe phases

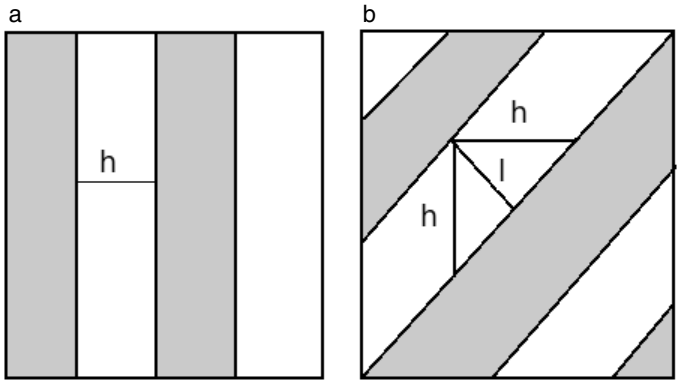

Figure 1. A schematic diagram of (a) the axial stripe phase of width h and (b) the diagonal stripe phase of width h; white regions have $\sigma = +1$ while gray regions have $\sigma = -1$.

as well as for rectangular phases, which they defined as a generalization of previously considered checkerboard phases [14]. The rectangular phases are described by Tang and Sun as consisting of 'rectangular domains with dimension $d_x \times d_y$; all magnetic moments within each rectangle align ferromagnetically, while moments in adjacent rectangles align antiferromagnetically' [13]. The main conclusion of their work was that there may be a region in phase space where, for a given ratio of dipole–dipole and exchange interaction, these rectangular phases become the ground state.

Returning to our model we can consider the phase behaviour as a function of J_s/g, for the chosen fixed ratio J/g. Extensive Monte Carlo simulations were conducted on a 2D square lattice, with $N = L^2 = 128^2$, which is larger than most previous simulations. Care was taken to allow sufficient initialization Monte Carlo steps (MCSs) to allow the system to reach equilibrium. This is very important as there are numerous metastable states, and this type of system can exhibit very slow non-equilibrium relaxation times [15, 16]. In a typical simulation 10^6–10^7 MCSs were used to equilibrate the system using an initial configuration from a simulation at a similar temperature. Data were then taken from a minimum of an additional 10^6–10^7 MCSs depending on the temperature. Statistically, the results presented are of better quality than those of Booth *et al*.

2. Results

2.1. Finite temperature simulations

As stated above the behaviour of a model monolayer has been studied extensively and has many interesting properties [9], which are a prime motivation for this current work. We have repeated and extended to larger system sizes the simulations reported by Booth *et al* [10] for a model monolayer with $J/g = 8.9$. Booth *et al* predicts that there is a second-order transition from a disordered phase into an ordered stripe phase at temperature $T_N/g \approx 5.1 \pm 0.1$. The nature of the ground state predicted by Booth *et al* is consistent with the predictions of a wonderful, analytic calculation by Giuliani *et al* [15]. Our simulation results are also all in agreement with those reported and the specific heat from our simulations is shown in both figures 2 and 3 as a line of small black squares for comparison.

To begin our study of the bilayer system we consider the case of a weak interlayer coupling. In figure 2 the specific heat calculated from extensive simulations for small values of the

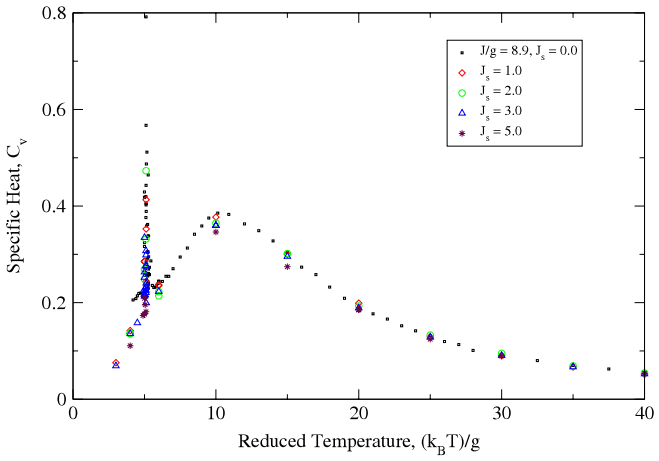

Figure 2. Specific heat as a function of temperature for weak interplanar exchange strength, J_s/g, with $J/g = 8.9$ and $N = 128^2$. The line of small black squares indicates the specific heat for a model monolayer.

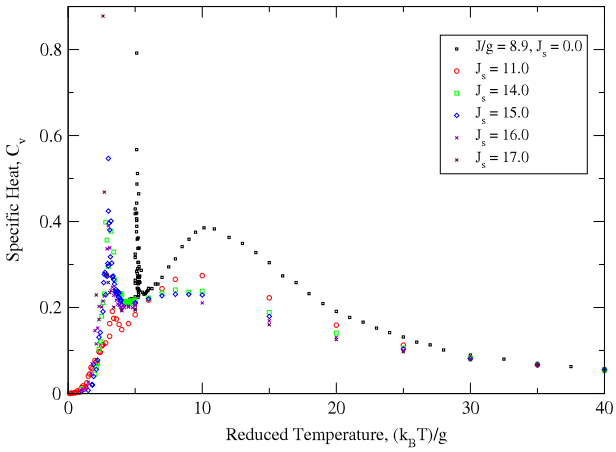

Figure 3. Specific heat as a function of temperature for intermediate interplanar exchange strength, J_s/g, with $J/g = 8.9$ and $N = 128^2$. The line of small black squares indicates the specific heat for a model monolayer.

interplanar coupling, $J_s/g = 1.0, 2.0, 3.0$, and 5.0, are shown. One can see that for these very small values of J_s/g there is little difference in the simulation results, when compared to the results for a monolayer. The statistical error in the points is comparable to the size of the symbols used. The transition temperature from the ordered phased to the disordered phase occurs at $T/g \approx 5.1 \pm 0.1$ over this range of J_s/g and the broad peak generally associated with the break-up of the extended domains occurs at $T/g \approx 10.0$, with a small, but systematic, reduction in the height. Only at approximately $J_s/g = 6.0$ does the Néel temperature begin to exhibit a dependence on J_s/g and T_N decreases as J_s/g increases. Direct observation of the spin configurations from these simulations indicates that the weak interplanar coupling does not change the nature of the phase transition. The low temperature ordered state remains axial stripes with a width of eight spins. In figures 4(a)–(c) typical spin configurations are shown for

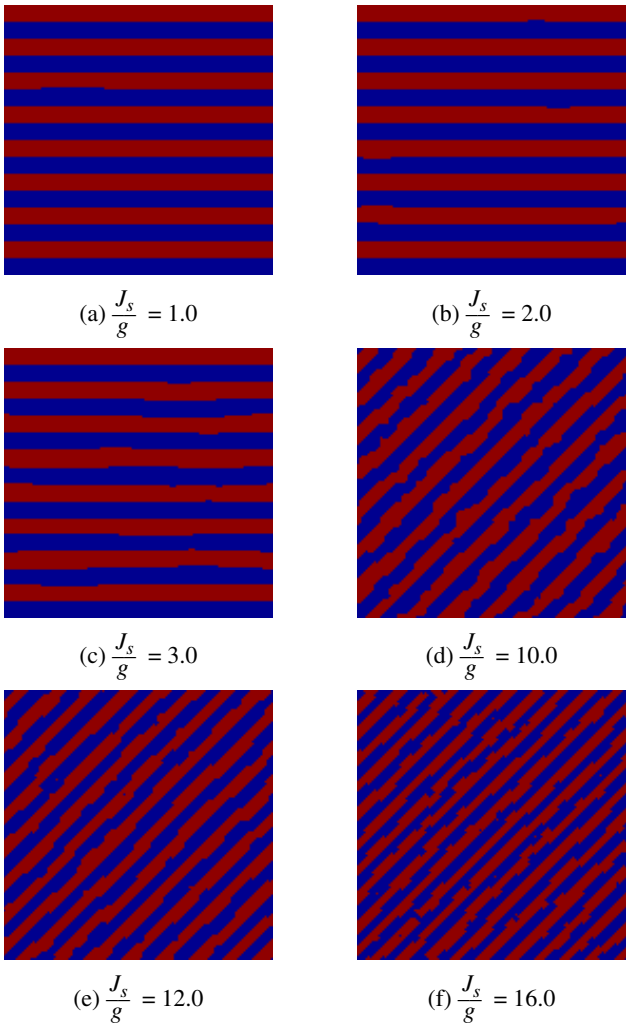

Figure 4. Typical equilibrium configurations for various J_s/g at temperature $T/g = 2.5$. Red/grey regions have $\sigma = +1$ while blue/black regions have $\sigma = -1$.

three such values of J_s/g at low temperature. The specific heat and direct observation of the configurations produced by the simulations show the evolution from the paramagnetic phase to the ordered striped phase as temperature is reduced, just as in the case of the monolayer. This is the case for values of J_s/g up to 8.0 ± 0.2.

We now consider larger values of the interplanar coupling. In figure 3 the specific heat is shown for both our results for a monolayer as well as the results for extensive simulations for $J_s/g = 11.0$, 14.0, 15.0, 16.0, and 17.0. In this figure one can see a significant difference between the bilayer and monolayer results. First the sharp transition at $T/g \approx 5.1$ has shifted to lower temperature and is an obvious function of J_s/g. One can see a substantial reduction in the height of the broad peak and a shift of the peak to lower temperature. More importantly, direct observation of the spin configurations generated in these simulations shows that the ground state of the model is no longer the striped phases as found by Booth *et al*. Figures 4(d)–(f) show three typical spin configurations from simulations with J_s/g in this regime at low temperature.

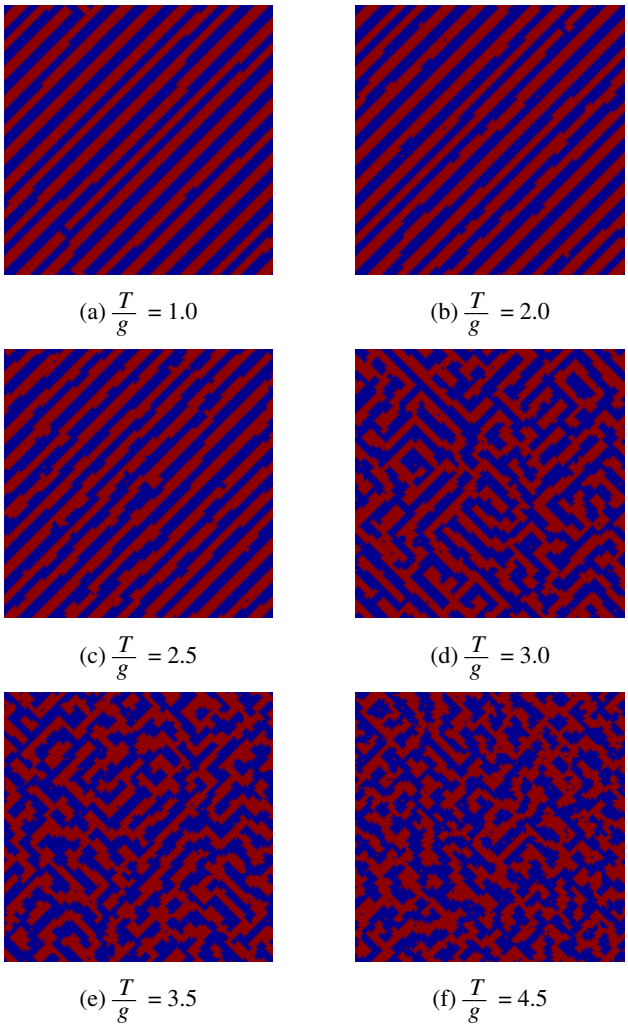

(a) $\frac{T}{g} = 1.0$ (b) $\frac{T}{g} = 2.0$

(c) $\frac{T}{g} = 2.5$ (d) $\frac{T}{g} = 3.0$

(e) $\frac{T}{g} = 3.5$ (f) $\frac{T}{g} = 4.5$

Figure 5. Typical equilibrium configurations for various T/g for $J_s/g = 16.0$. Red/grey regions have $\sigma = +1$ while blue/black regions have $\sigma = -1$.

Further, figure 5 shows six snapshots of typical spin configurations from a simulation with $J_s/g = 16$ in various temperature regimes. One can see from the configurations that the system has formed an ordered stripe phase, but, rather than stripes along the lattice axes, the stripes are along the diagonal of the underlying lattice. One can still see a similar succession of phases from this orientationally ordered stripe phase, to a phase with stripes along both $x = y$ and $x = -y$, and finally, at high temperature, a completely disordered phase. It is important to note that the spins remain uniaxial and perpendicular to the film. What is observed is a rotation of the stripes, not a rotation of the spins.

The change in the nature of the ordering and changes in the stripe width can be tracked by using the two-dimensional structure factor;

$$S(q_x, q_y) = \langle |\sigma(q_x, q_y)|^2 \rangle, \tag{3}$$

where $\sigma(\vec{q})$ is the discrete Fourier transform of the spin system, $\sigma(\vec{r})$. Figures 6–9 show

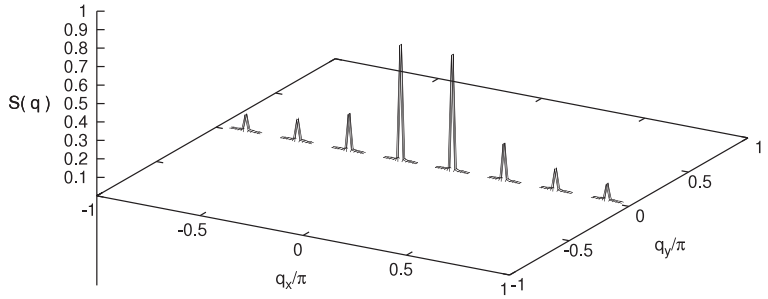

Figure 6. The structure factor for $J_s/g = 3.0$ at temperature $T/g = 2.5$. All values below 0.01 have been excluded to more clearly show the peaks.

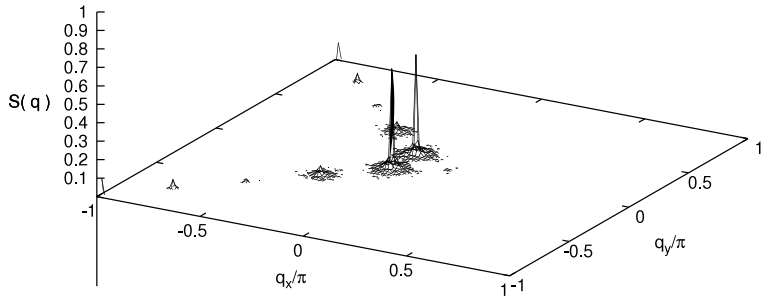

Figure 7. The structure factor for $J_s/g = 10.0$ at temperature $T/g = 2.5$. All values below 0.01 have been excluded to more clearly show the peaks.

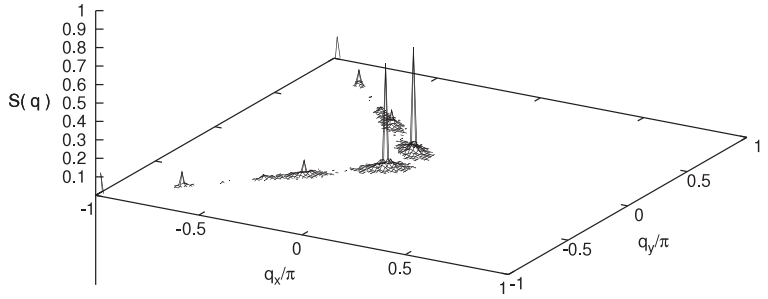

Figure 8. The structure factor for $J_s/g = 12.0$ at temperature $T/g = 2.5$. All values below 0.01 have been excluded to more clearly show the peaks.

$S(q_x, q_y)$ as calculated at four points in phase space, all at a temperature of $T/(k_B g) = 2.50$ in reduced units. A typical configuration at each of these four points in phase space is shown in figure 4. Note that we take advantage of the symmetry of q-space to shift $\vec{q} = 0$ to the centre of figure, and to more clearly show the peaks in the structure factor we do not plot any points with a magnitude lower than 0.01. For $J_s/g = 3.0$ the main peaks in the structure factor occur at $\vec{q} = (0, \pm\frac{\pi}{8})$ as one would expect for axial stripes of width eight oriented parallel to the x-axis. For $J_s/g = 10, 0, 12.0$, and 16.0 we see peaks at $\vec{q} = (\frac{-7\pi}{64}, \pm\frac{7\pi}{64})$, $\vec{q} = (\frac{-8\pi}{64}, \pm\frac{8\pi}{64})$, and $\vec{q} = (\frac{-10\pi}{64}, \pm\frac{10\pi}{64})$ respectively. Note that the peaks all occur along the diagonals of q-space, indicating that the characteristic lengths in the x and y direction in real space are equivalent. The location of the main peaks along the diagonals in q-space indicates

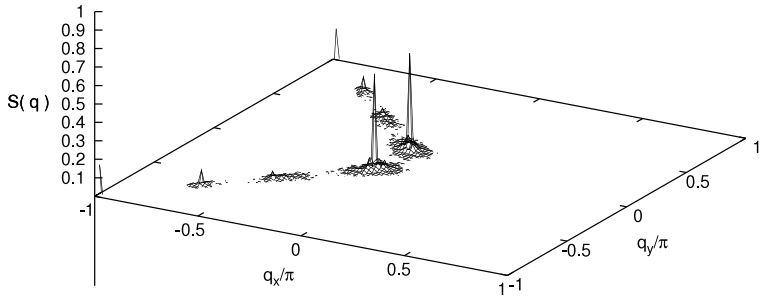

Figure 9. The structure factor for $J_s/g = 16.0$ at temperature $T/g = 2.5$. All values below 0.01 have been excluded to more clearly show the peaks.

that this characteristic length is decreasing as J_s/g increases. The magnitudes of the main peaks in the figures become smaller as J_s/g increases due to the decrease in T_N as a function of J_s/g; therefore, $T/(k_B g) = 2.50$ is closer to the Néel temperature as J_s/g increases.

This region of stability for rotated stripe phases is due to the additional, interplanar frustration introduced by the pure antiferromagnetic sublayer. When the upper layer is ordered with axial stripes, one-half of the bonds with the lower layer must be unsatisfied. For a weak interplanar exchange coupling, the frustration between the intraplanar dipole–dipole and exchange interactions still defines the ground state for the system. However, as J_s/g is increased, the strength of the interplanar frustration grows, until at some critical value of J_s/g the stripes rotate. By doing so the interplanar frustration is reduced as all bonds along the now diagonal stripe interface (along lines parallel to the $x = y$ or $-y$ axes) are satisfied between the two layers. The intraplanar frustration is still significant, and initially the stripe width observed is comparable to that observed in the monolayer. As J_s/g is further increased the system seeks to further minimize the interplanar frustration by introducing more diagonal interfaces in the upper layer by reducing the stripe width. A technical point is that this leads to problems with commensurable stripe widths as seen in simulations of stripes in the monolayer [10, 12, 17]. The reduction in diagonal stripe width continues until one reaches stripes of width three. As we will show later, this reduction in stripe width also leads to a reduction in the Néel temperature as one would expect.

We have not seen a reference to rotated stripe phases in the literature, although they do appear qualitatively similar to that predicted for Mn/Ag(111) by Heinze [18], but that analysis is based on the hexagonal lattice of Mn/Ag.

It is important to note that the rotated stripe phase observed in our simulations is not the same as the rectangular phases predicted by Tang and Sun [13]. For small stripe width, with some thermal disorder, the two phases can appear superficially to be similar; however, they are quite distinct classes of phases and have distinct structure factors. In this current work we have seen rotated stripes of width up to eight spins. Rectangular phases with an equivalent scale have not been observed in our simulations.

The expectation was that as J_s/g was increased further the system would eventually order in diagonal stripes of width one, which is geometrically equivalent to the pure antiferromagnetic or AA phase. Initial simulations supported this conjecture somewhat, but the very low transition temperatures measured and the number of metastable states in this region of phase space made it necessary to conduct very extensive simulations, where one was careful to check that the system remained in equilibrium and was not stuck in a metastable state. These simulations revealed the existence of a small region of stability for an intermediate phase between the

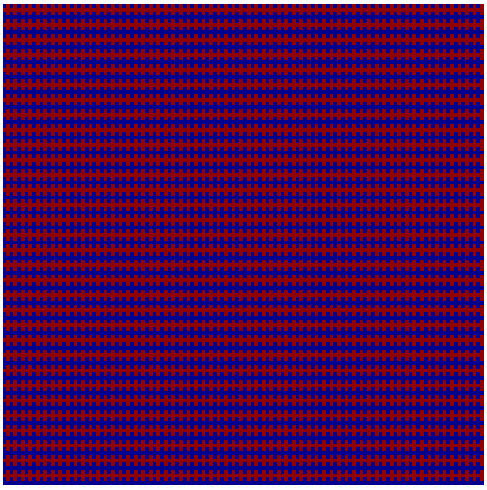

Figure 10. The zipper phase. Red/grey regions have $\sigma = +1$ while blue/black regions have $\sigma = -1$.

diagonal stripes and the AA phase. Figure 10 shows a sample of the perfectly ordered phase, which we refer to as the zipper phase. This state is best considered as a modification of the AA state due to the frustration of the intraplanar interactions. Every second line in the zipper phase is ordered antiferromagnetically along one axis and matches the lower layer. The other half of the lines in the system are ordered ferromagnetically along this axis such that half of the spins have unsatisfied bonds with the lower layer. The state of these ferromagnetic lines of spins alternates between $\sigma = +1$ and -1. Thus three-quarters of the interlayer bonds are satisfied and one-quarter are frustrated. In the ordered state the lines of antiferromagnetically and ferromagnetically ordered spins occur only along one lattice axis, while above the T_N one is able to observe these structures along both axes.

For still larger values of the interplanar coupling one finds that there is a continuous change from the disordered phase to the AA phase, where the upper layer matches the antiferromagnetic ordering of the static lower layer. Figure 11 shows the specific heat for a system at $J_s/g = 35.0$ as a function of temperature for various size lattices. The lack of finite size effects would indicate that this is a first order transition.

2.2. Zero temperature

One can calculate the energy of the various phases observed at low temperatures in the simulations and determine which has the lowest energy and might be expected to form the $T = 0$ ground state. We can do this for axial stripes of width eight spins along the lattice axis, for phases with stripes along the diagonal, for the zipper phase and for the AA phase. The width of a diagonal stripe can either be characterized as the length of the line perpendicular to the line $x = y$ (or $x = -y$) as shown by l in figure 1(b), but a more convenient measure is to take the width as the number of spins parallel to the x or to the y axis. This is given in figure 1(b) by h. In terms of the width h only diagonal stripes with odd width will have an energy dependent on J_s/g. The energy of axial stripe phases does not depend on J_s/g regardless of the stripe width. The energies of the relevant phases, with $J/g = 8.9$, are shown in figure 12.

One sees that the axial stripe phase of width $h = 8$ has the lowest energy for $J_s/g < 11.3 \pm 0.1$, at which point the energy of the diagonal phase with $h = 7$ becomes lower. At

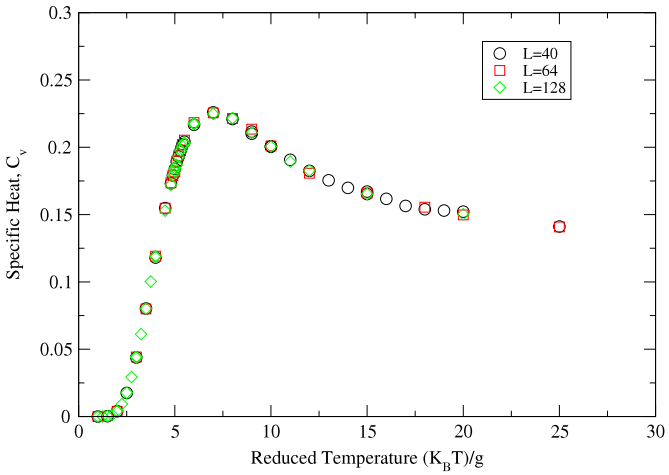

Figure 11. Specific heat as a function of temperature for $J_s/g = 35.0$ at $J/g = 8.9$ for various system sizes; $N = 40^2, 64^2, 128^2$.

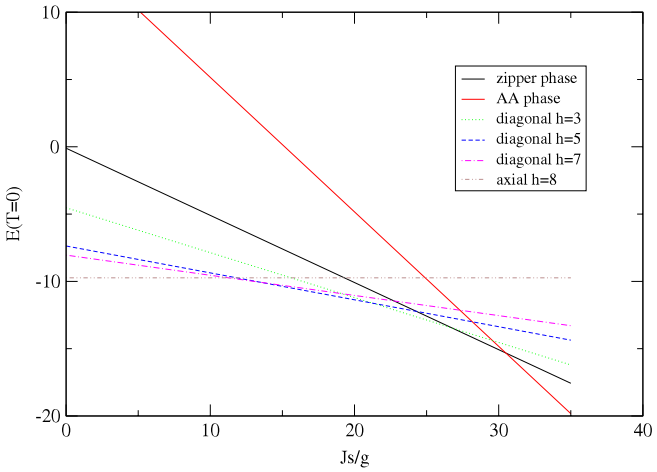

Figure 12. The variation of the energy with J_s/g for axial stripes of width $h = 8$, diagonal stripes of width $h = 7, 5, 3$, the zipper phase and the AA phase.

$J_s/g = 13.6 \pm 0.1$ the diagonal stripes with $h = 5$ have the lowest energy; at $J_s/g = 21.3 \pm 0.1$ the diagonal stripes with $h = 3$ become the lowest-energy phase. The energy of the zipper phase varies as $-\frac{1}{2}J_s/g$ and is the lowest-energy phase for $26.6 \pm 0.1 < J_s < 30.5 \pm 0.1$. Finally, for $J_s/g > 30.5 \pm 0.1$ the AA phase (which is equivalent to diagonal stripes of width $h = 1$) becomes the ground state. These changes in the lowest-energy phase are all consistent with the results of the finite-temperature simulations.

2.3. Phase diagram

One can combine the results of the simulations with the $T = 0$ calculations and derive a proposed phase diagram for the model system. Such a diagram is given in figure 13, where five regions have been identified: axial stripes, diagonal stripes, the zipper phase, the AA phase and

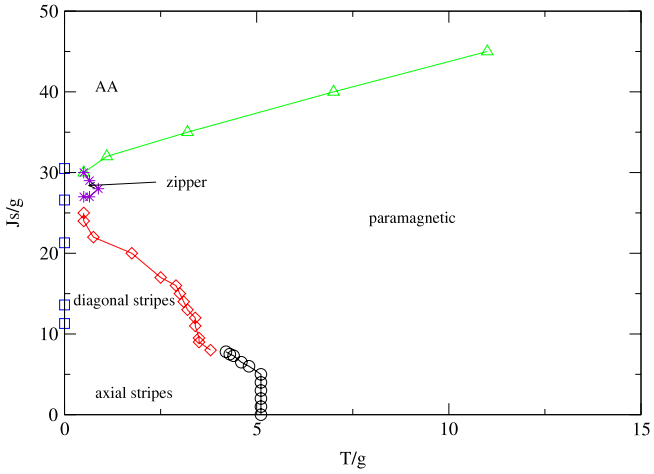

Figure 13. Proposed phase diagram for the model magnetic bilayer. Circles indicate a transition to an axial stripe phase. Diamonds indicate a transition to a diagonal stripe phase. Stars indicate a transition to the zipper phase. Triangles indicate a transition to the AA phase. Squares indicate a change in the lowest-energy phase as discussed in the text.

the paramagnetic phase. The lines in the figure are estimates of the phase boundaries formed by connecting the simulation data points for transitions to similar ordered states. The circles on the phase diagram are the data points from the simulations where the system orders into an axial stripe phase. The diamonds are the transition points where the system orders into a diagonal stripe phase. The stars indicate transitions into the zipper phase and the triangles are transition points where the system orders in the AA phase. The squares are the zero-temperature estimates based on the energies calculated above. A determination of the low-temperature phase boundaries, between the ordered phases, will require even more extensive simulations, and therefore we have chosen not to include estimates for these phase boundaries in figure 13.

For low values of the interplanar exchange coupling, J_s/g, the axial stripe phase is the stable phase at low temperature. As the temperature is increased one observes the phase transition to the tetragonal phase defined by Booth *et al*, which then disorders at high temperature. One can determine the location of the phase transition by tracking either the specific heat or by calculating the orientation order parameter defined by Booth *et al* [10],

$$O_{\mathrm{hv}} = \frac{n_{\mathrm{h}} - n_{\mathrm{v}}}{n_{\mathrm{h}} + n_{\mathrm{v}}}, \tag{4}$$

where n_{h} and n_{v} are the number of bonds between spins with opposite orientations which are parallel to the horizontal or vertical direction, respectively.

For intermediate values of J_s/g, the low-temperature state is the newly defined diagonal striped phase where the width of the phases depends on the strength of the interplanar exchange, J_s/g. In our simulations we observe stripe widths from $h = 7$ down to $h = 3$. Much as in the case of the axial stripe phase, as the temperature is increased there is a transition to a tetragonal phase with stripes along both diagonals. This phase transition is indicated by the peak in the specific heat and can also be seen in the structure factor. Below T_{N} there are two main peaks in $S(\vec{q})$ along one set of the diagonals in q-space, characteristic of diagonal stripes along one of the diagonals in real space: either $y = x$ or $-x$. At T_{N} and above there are four main peaks in $S(\vec{q})$, as one has diagonal stripes along both diagonals in real space. If one defines $\vec{q}_+$ and $\vec{q}_-$ as the locations of the main peaks in q-space associated with diagonal stripes along $x = y$ and

$x = -y$ respectively, then one can define a general order parameter,

$$O_{\pm} = \left\langle \frac{|S(\vec{q}_{+}) - S(\vec{q}_{-})|}{(S(\vec{q}_{+}) + S(\vec{q}_{-}))} \right\rangle, \tag{5}$$

which will be non-zero below T_{N} with a saturation value of one and zero above. The Néel temperature is reduced as J_s/g increases due to the decreasing stripe width in the ordered state. The thermal energy required to introduce defects into the stripe pattern is smaller for thinner stripes. As the temperature increases the tetragonal phase decays into the paramagnetic phase.

Determining the value of J_s/g at which the ordered state changes from axial to diagonal stripes has proven to be quite difficult. Simulations place the transition near $J_s/g = 8.0 \pm 0.2$, but as one can see from the proposed phase diagram $\partial T_{\mathrm{N}}/\partial J_s$ has a very large, negative slope as J_s/g approaches this point. This steep slope and the normal systematic errors associated with Monte Carlo simulations are responsible for the difficulty in providing a better estimate for this critical point.

At $J_s/g = 26.6 \pm 0.1$ the ground state becomes the zipper phase. In this region of phase space T_{N} is small relative to the size of the various interactions and there are a number of metastable states. Great care must be taken to insure the simulation remains in equilibrium; however, the transition is very sharp and can be seen clearly via the specific heat or by using the structure factor.

Finally, for large values of the interplanar exchange, $J_s > 30.5 \pm 0.1$, the ground state is the AA phase. As J_s/g gets larger the transition temperature grows linearly. A least squares fit to the transition temperatures calculated for $J_s/g = 32, 35, 40$ and 45 yields $T_{\mathrm{N}}/g \approx -23.43 + 0.764(J_s/g)$.

Characterizing the nature of the transitions between the various phases can be quite difficult. As in the case of the monolayer it is difficult to determine whether the transition from the disordered tetragonal phase to the stripe phases, axial or diagonal, is continuous or weakly first order. This will require much more extensive consideration. The transition to the zipper phase and the AA phase, for large values of the interplanar coupling, J_s/g, appears to be first order in both cases. The transitions at low, fixed temperature between the ordered phases also appear, from finite size effects, to be first order. However, this analysis is not conclusive and again it will require more extensive simulations to provide a definitive answer as to the order of these transitions.

3. Summary

We have derived the phase diagram for a model magnetic bilayer system as a function of temperature and interplanar exchange strength in a region of phase space of potential technological interest. We considered an upper magnetic layer with spins perpendicular to the film which interact via a long-range dipolar interaction and a short-range exchange interaction and which is coupled to a static, pure antiferromagnetically ordered lower layer by an interplanar exchange interaction. The stripe phases found in the related monolayer system remain for weak couplings, but a novel rotated stripe phase is observed for moderate values of the interplanar exchange coupling. For these intermediate values the stripes are rotated such that they lie along one of the diagonals of the lattice. The stripe width and the Néel temperature both decrease as the strength of the interplanar coupling increases. There is also a small region where a zipper phase is stable. The zipper phase is a modification of the AA phase, where every second line of spins along one axis (x or y) is ferromagnetically ordered. The state of the ferromagnetic lines of spins alternates between the $+1$ and -1 states. For large values of the interplanar exchange the system orders in the AA phase.

Acknowledgments

This work was supported by the Natural Sciences and Engineering Council of Canada (NSERC). The authors would like to acknowledge SHARCNET for the provision of the computing resources used in this work.

References

[1] Jensen P J and Bennemann K H 2006 *Surf. Sci. Rep.* **61** 129
[2] Prinz G A 1998 *Science* **282** 1660
[3] Wolf S A, Awschalom D D, Buhrman R A, Daughton J M, von Molnár S, Roukes M L, Chtchelkanova A Y and Treger D M 2001 *Science* **294** 1488
[4] Takano K, Kodama R H, Berkowitz A E, Cao W and Thomas G 1997 *Phys. Rev. Lett.* **79** 1130
[5] Ohldag H, Scholl A, Nolting F, Arenholz E, Maat S, Young A T, Carey M and Stöhr J 2003 *Phys. Rev. Lett.* **91** 017203
[6] Hellwig O, Kirk R L, Kortright J B, Breger A and Fullerton E E 2003 *Nat. Mater.* **2** 112
[7] Venus D and Hunte F 2005 *Phys. Rev.* B **72** 024404
[8] Ali M, Adie P, Marrows C H, Greig D, Hickey B J and Stamps R L 2007 *Nat. Mater.* **6** 70–5
[9] De'Bell K, MacIsaac A B and Whitehead J P 2000 *Rev. Mod. Phys.* **72** 225–7
[10] Booth I N, MacIsaac A B, Whitehead J P and De'Bell K 1995 *Phys. Rev. Lett.* **75** 950–3
[11] Arlett J, Whitehead J P, MacIsaac A B and De'Bell K 1996 Phase diagram for the striped phase in the two-dimensional dipolar Ising model *Phys. Rev.* B **54** 3394–402
[12] MacIsaac A B, Whitehead J P, Robinson M C and De'Bell K 1995 *Phys. Rev.* B **51** 16033–45
[13] Tang B and Sun G 2002 Striped and rectangular phases in multilayered Ising systems with dipolar interaction *Phys. Rev.* B **65** 132418
[14] Czech R and Villain J 1989 *J. Phys.: Condens. Matter* **1** 619
[15] Giuliani A, Lebowitz J L and Lieb E H 2006 *Phys. Rev.* B **74** 064420
[16] Bromley S P, Whitehead J P, D'Bell K and MacIsaac A B 2003 *J. Magn. Magn. Mater.* **264** 14
[17] MacIsaac A B, Whitehead J P, De'Bell K and Sowmya Natayanan K 1992 Monte Carlo study of two-dimensional Ising dipolar antiferromagnets as a model for rare-earth ordering in the R–BA–Cu–O compounds (R = rare earth) *Phys. Rev.* B **46** 6387–94
[18] Heinze S 2006 *Appl. Phys.* A **85** 407